# Operational Bias Correction of Hourly Radar Precipitation Estimate using Rain Gauges

Roberta Amorati, Pier Paolo Alberoni, Anna Fornasiero

*Servizio IdroMeteoClima ARPA Emilia-Romagna, viale Silvani 6, I-40122 Bologna, Italy.*
ramorati@arpa.emr.it
(Dated: 30 May 2012)

Roberta Amorati

## 1. Introduction

The radar estimate of precipitation is recognized to be of great value for operational use, the high spatial and temporal resolution being a key point in nowcasting procedures. It is also well known that the radar precipitation estimate suffers for different sources of error that have to be removed in order to fulfill meteorological and hydrological requirements. First of all reflectivity corrections are necessary, but benefits may be achieved by blending other sensor measurements (see among the others Chumchean et al., 2006).

Merging the radar estimate with precipitation observed by a dense rain gauge network seems to be a solution. On the other side, often the merging techniques are not only inadequate, but even misleading. The correction by means of a sparse network has to take into account the complexity of the precipitation field itself and instrument limits that may lead to a non-uniform bias field, particularly in areas with complex orography. Moreover different precipitation regimes originate different bias field structures, convective events being very intermittent in time and space. Many techniques have been proposed with different degrees of complexity, some to remove mean bias, some other to reconstruct the bias field, to geostatistical methods. (Barbosa, 1994; Goudenhoofdt and Delobbe, 2009).

In this work it is investigated the performance of a real time algorithm for mean radar bias correction and it is compared to an algorithm that reproduce the non uniform bias correction hourly. The test is conducted over a two months period, where convective, and mixed large scale convective events take place.

## 2. Data

### *a) Radar Quantitative Precipitation Estimate*

For this study hourly precipitation estimates by a single radar are used. The instrument is managed by ARPA-SIMC and it is located in a flat area of Po Valley at 44.6547° Latitude and 11.6236° Longitude; the Alps are about 120 km northward, the Apennines are about 50 km southward and the Adriatic Sea is about 60 km eastward.

The actual scheme used at ARPA-SIMC to correct radar data and to provide rain rate estimates operatively is composed by:

- mean clutter reduction, performed through static maps of elevations recorded in dry weather : for each azimuth-range pair is considered the reflectivity measure at the first elevation not affected by mean clutter;
- dynamic clutter reduction, obtained by means of beam trajectory simulation, a DEM and radiosounding information (Fornasiero et al., 2006);
- beam blocking reduction and correction based on a geometric-optic approach (Bech et al., 2003, Fornasiero et al. 2006);
- anomalous propagation detection, realized analyzing the echo coherence in the vertical direction (Alberoni et al., 2001);
- Z-R conversion: a relation of type $Z=aR^b$ is used, whit standard coefficient a=200 and b=1.6.

The precipitation rate at the ground is then interpolated from polar coordinates to a 256 X 256 Cartesian grid of 1km X 1km resolution.

Rain rates are obtained every 15 minutes and the final rain total over a 1-hour period is computed by an advective algorithm taking into account the movement of precipitating systems. The algorithm is based on the computation of maximum cross-correlation between consecutive maps, leading to the estimate of the displacement vector for each precipitation system. The precipitation field is then reconstructed every minute between the observed maps and finally cumulated over one hour.

### *b) Rain gauge network*

The rain gauge network is composed by more than 400 instruments that produce hourly cumulated rain amount. More than 200 lie on the 125 km range radar areas, located mainly over river basins and urban areas. The complete set is split in two parts, one used for the merging procedures, the other for verification.

*c) Case studies*

For this work, two months of hourly precipitation data is used, from the 1st of September to the 31st of October 2010. During that period 11 days of purely convective precipitation were identified and 12 days of convection embedded in stratiform precipitation and triggered by a large scale system took place.

## 3. Blending radar-gauges methods

The merging techniques use pairs of radar and gauge precipitation, obtained taking the median of the nine radar pixels surrounding the gauge location. For every *i*-th gauge, a radar $R_i$ a and rain gauge $G_i$ precipitation values are given.

*a) Mean Bias Removal*

For every instant *t* the points having both radar and rain gauge measurements greater than 0.2 mm are selected. For this dataset, it is calculated

$$\log F_{i,t} = \log_{10}\left(\frac{G_{i,t}}{R_{i,t}}\right)$$

and a mean value is given by

$$\log F_t \equiv \overline{\log F_{i,t}} = \frac{1}{N_t}\sum_{i=1}^{N} \log F_{i,t} \quad , \quad N_t = \text{number of available points at time } t$$

The mean is a good estimator under the assumption that the *logF* distribution is normal (*F* log-normal distributed). This assumption holds when the sample size is increased. In Fig. 1 the histograms for an hour and a four days period are shown.

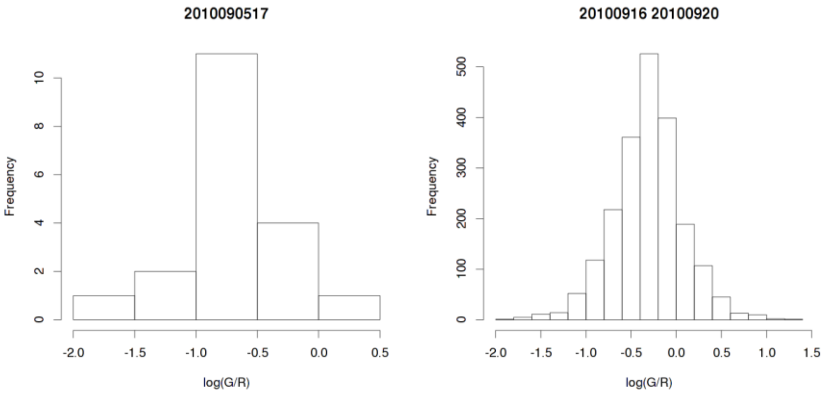


*Fig. 1 Histograms of hourly logF relating to an hour dataset (left) and to a four days dataset (right)*

If x = log(G/R) and $\bar{x}$ is the mean, the variable z = x - $\bar{x}$ is unbiased, as it has a null expected value.

Defining $F \equiv 10^{\bar{x}} \Leftrightarrow z = \log\frac{G}{R} - \log F = \log\frac{G}{RF}$, so that variable *R'*=*RF* generates an unbiased G/ *R'* distribution.

The F value can be used to remove the mean bias from the radar hourly precipitation maps.

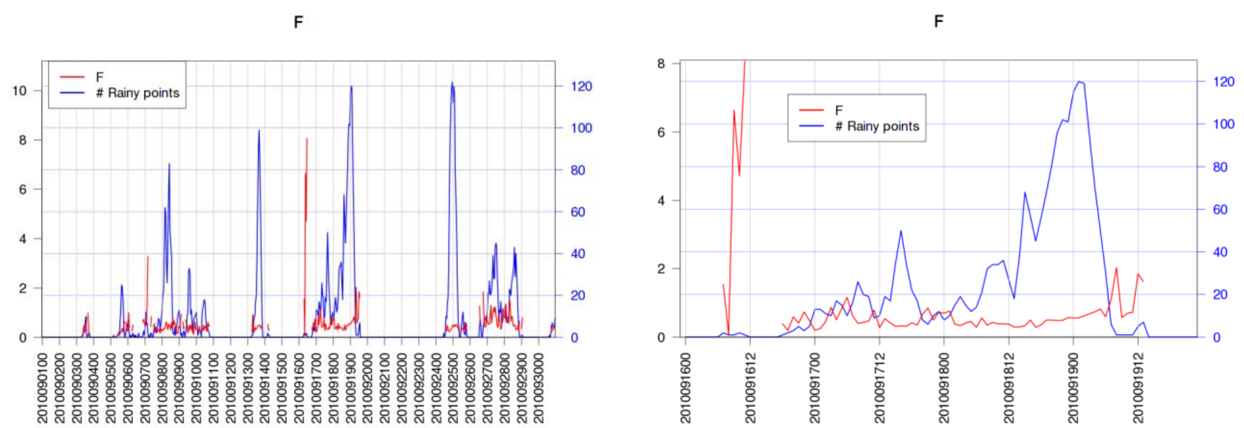


*Fig 2. Time series of hourly F bias correction factor. On the left: from the 1st to the 30th of September 2010 and on the right from the 16th to the 19th of September 2010.*

In Fig.2 it is shown the time series of F values computed hourly. The blue line describes the number of rainy points used for the computation and ranges from 0 for dry days up to 120 for rainy instants. The number of available points for the computation of the factor F varies widely from one hour to the next and causes F to change very rapidly (red curve). The oscillation is stronger when the sample $N_t$ is low and the instability of the mean is higher. In the left panel of Fig. 2 the trend during September is put in evidence and it can be noticed that F is lower than 2 for almost all the time while some higher peaks can be seen on the 7$^{th}$ and 16$^{th}$. On the right panel of Fig.2 a close-up of the period from the 16$^{th}$ to the 19$^{th}$ is pointed out. The peak on the 16$^{th}$ reaches the value of 8 and is associated to a very poor sample of data. During the rest of the period F ranges from close to 0 to about 2. The pattern observed for September is observed also for the October dataset (not shown). The high variability from one instant to the next produces a discontinuity of the correction factor that leads to a difficult real-time operational use of precipitation radar maps. If the aim of the correction is removing the mean bias produced by radar components, neglecting intrinsic variability of the precipitation fields, the stability of correction factor can be improved by increasing the time range of data aggregation. A four days time aggregation period Δt is then considered and the mean of logF is computed as follows:

$$\overline{logF_t} = \frac{\sum_{\tau=t-\Delta t}^{t} \sum_{i=1}^{N_\tau} logF_{i,\tau}}{\sum_{\tau=t-\Delta t}^{t} N_\tau}$$, $N_\tau$ = number of available points at time τ

At each instant t, the F correction factor is computed using a four days record of radar-gauge pairs. This process requires a warm-up time at the end of long dry periods and produces peaks when precipitation rapidly decays, anyway it greatly stabilizes the hourly F trend. In Fig. 3 the red curve represents F values as in Fig.2, but computed using four days record. The spikes are no more present and the range of variability is very lower (notice the y-axis scale).

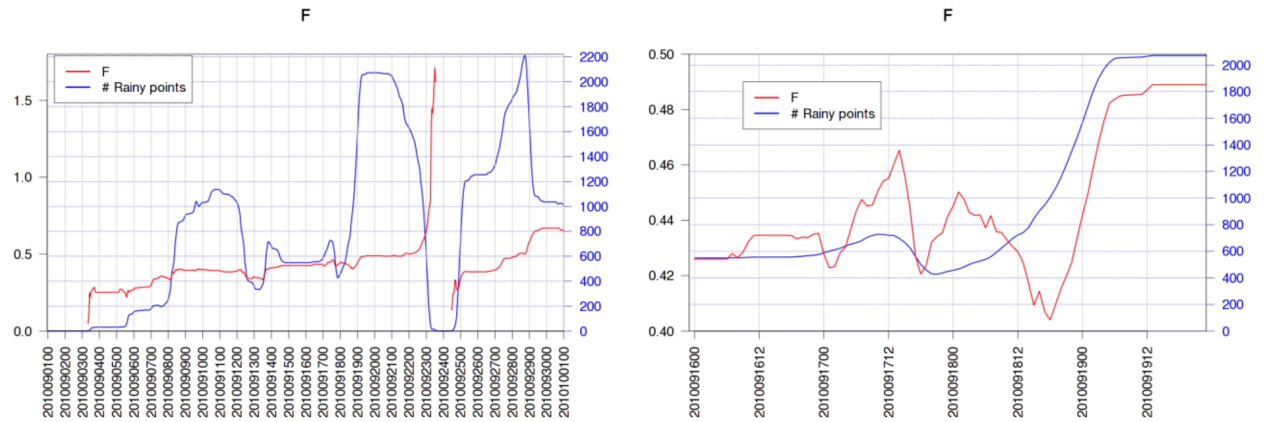


*Fig 3. Same as Fig. 2, F calculated using a record of 4 days .*

In this work, the radar precipitation hourly maps are corrected using F calculated hourly with a four days record.

*b) Non-uniform Bias Correction*

The merging method for the reconstruction of non-uniform bias correction maps is a modification of that one proposed by Koistinen and Puhakka (1981) (hereafter K&P) that draws on that of Brandes (1975). The K&P method produces fields of correction factor combining a term depending on rain gauge density and a term depending on distance from the radar.

In the present work, the aim is the correction of 1km x 1km resolution hourly precipitation radar fields. For these time and space resolutions the range dependence was preliminary investigated in our target area for the whole 2010 year dataset. In that experiment the correlation of log(G/R) versus the distance from radar was found to be very low. Then, in the present work, only the term depending on rain gauge density is considered.

For each pair of gauge and radar measurements a threshold of 1mm is used to select rainy points, and at least ten points are required. This value allows to eliminate the high variability of log(G/R) for small values that introduces instability in the field of corrections factor.

For each rainy point *g*, $F_g = \frac{G_g}{R_g}$ is computed and for every pixel (*i,j*) the correction is given by $F_{i,j} = \frac{\sum_{g=1}^{N} w_{g,ij} F_g}{\sum_{g=1}^{N} w_{g,ij}}$.

$w_{g,ij}$ is the weight that the observation *g* receives for the grid point *(i,j)* and it is given by $w_{g,ij} = \frac{1}{4\pi k}\exp\left(-\frac{r_{g,ij}^2}{4k^2}\right)$, $r_{g,ij}$ is the distance from point *g* to the grid point *(i,j)* and *k* is a filter parameter that depends on grid point *(i,j)* and is taken as $k_{ij} = \sqrt{A_5/5}$, where $A_5$ is the area containing the nearest 5 stations. Once the correction field $F_{ij}$ is calculated, the radar grid of precipitation $R_{ij}$ is corrected point by point giving a new hourly precipitation map: $R'_{ij}=R_{ij}F_{ij}$

In Fig. 4 an example of non-uniform bias correction process for hourly precipitation is shown. It is to notice that the maximum variability of F is concentrated in the up-left region of the radar circle, where the density of gauge measurements is high and precipitation is heavy. The precipitating system on the West is increased by the correction, while the precipitation on the South-East area is decreased.

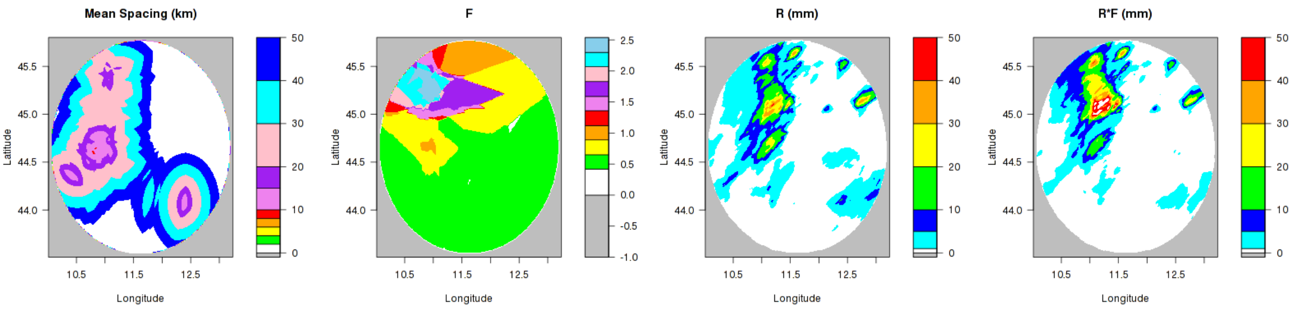


*Fig 4. Example of non-uniform bias correction steps relative to 2010-09-08 05UTC. From left to right: $F_g$ mean spacing (km), F field, radar precipitation map and radar corrected precipitation map.*

## 4. Discussion and results

Both correction techniques described in *3-a* (hereafter BSRM) and *3-b* (hereafter ADJ) are applied to the target dataset described in *2-c*. Verification of performances is done versus a set of more than 100 independent rain gauges, coupling each rain gauge to the corresponding radar grid precipitation estimate.
On the left side of Fig. 5 (*a*, *c* and *e* panels) the results from 2010-09-18 00 UTC to 2010-09-20 00 UTC (hereafter: case 1) and on the right side (*b*, *d* and *f* panels) the results from 2010-10-04 00 UTC to 2010-10-06 00 UTC (hereafter: case 2) are given.
In these graphs, patterns of some distribution parameters are shown: mean, median and 95° percentile (95%). The x axis is time at 1h steps. At every instant, the mean, the median and the 95% are computed for the separated distributions; the blue line represents gauges, the red line radar RAW, the orange line BSRM and the purple line ADJ.
In case 1, the radar RAW overestimates with respect to gauges almost all the time. The radar BSRM is very lower than radar RAW and close to the gauges with the median. The 95%, and hence the mean, are lower than the corresponding gauge parameters. This behavior is probably due to a strong reduction operated by the BSRM algorithm, more significant for heavy precipitation. The overestimation persists for radar ADJ, anyway it is closer to the gauges curve than radar RAW, for all the parameters and for almost all the time. In case 2, radar RAW overestimates the median, underestimates the 95% and the mean is close to the gauges curve. A 3 hours shift of the maximum of precipitation is evident. As in case 1, the BSRM algorithm reduces strongly the radar precipitation and it is shown by all the parameters. The ADJ reduces the median of radar distribution for almost all the time, in some instants it increases the mean and 95% and in others it decreases them.

Commonly used statistical indices are also considered for the verification: *bias*, mean absolute error (*mae*) and root mean square error (*rmsq*). These are computed for the whole dataset (i.e. from 2010-09-01 to 2010-10-31) and results are summarized in Table 1. The bias varies from a positive value for radar RAW to a negative value for BSRM and it is closer to zero for ADJ. Mae is decreased by both BSRM and ADJ algorithms with respect to radar RAW and has similar values. The rmse decreases from RAW to BSRM and ADJ.

| | **BIAS** | **MAE** | **RMSE** |
|---|---|---|---|
| **Radar RAW** | 0.644 | 1.072 | 2.357 |
| **Radar BSRM** | -0.246 | 0.692 | 1.833 |
| **Radar ADJ** | 0.195 | 0.633 | 1.597 |

*Table 1. Statistical indices*

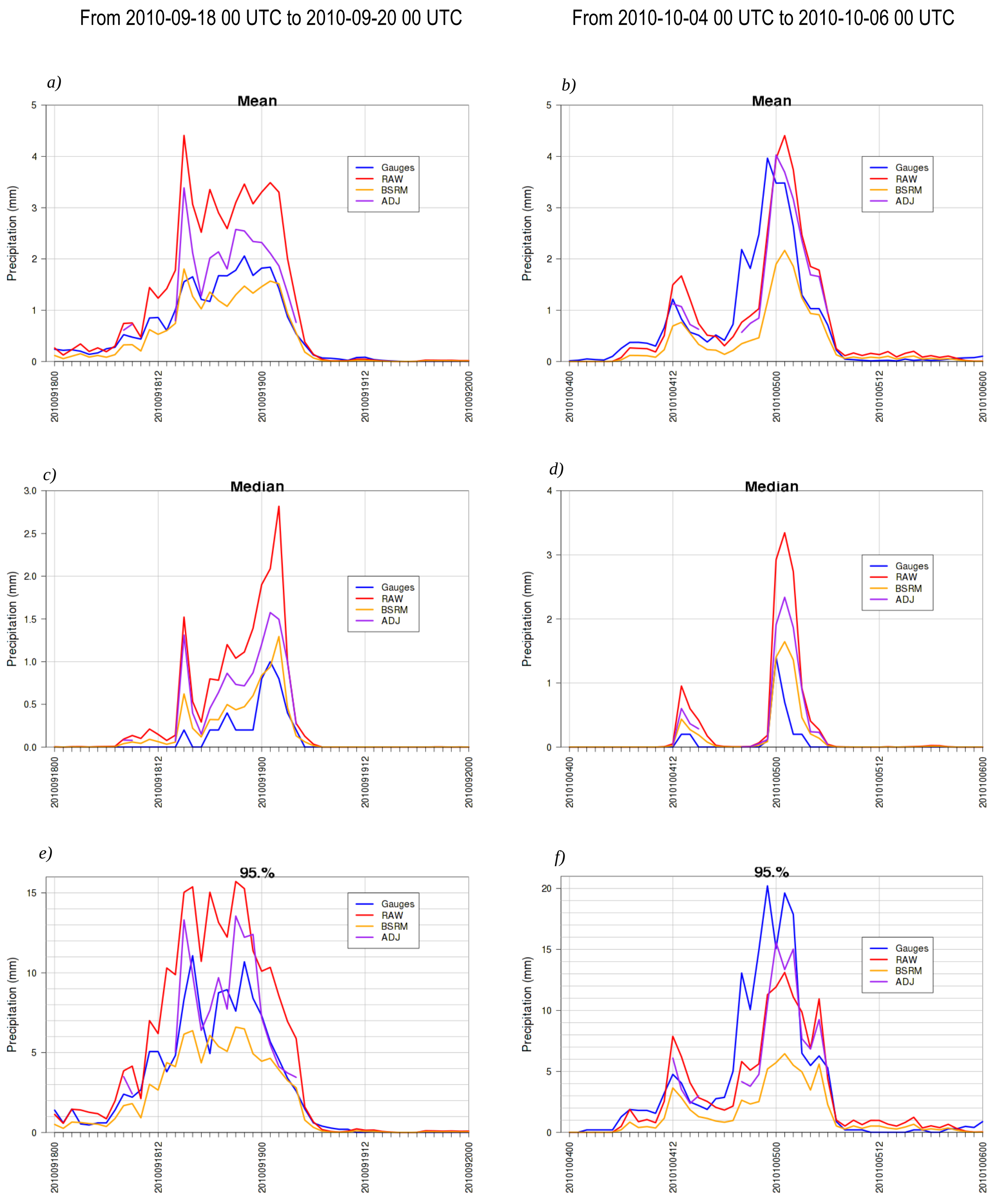


*Fig. 5. Mean (*a *and* b panels*), median (*c *and* d panels*), and 95% (*e *and* f panels*). The results are from 2010-09-18 00 UTC to 2010-09-20 00 UTC (*a, c *and* e panels*) and from 2010-10-04 00 UTC to 2010-10-06 00 UTC (*b, d *and* f panels*)*

## 5. Summary and conclusion

In this work two simple techniques for blending rain gauges measurements and radar quantitative precipitation estimates are explored, in order to evaluate the possible use in operative procedures. The test is conducted for two months of hourly cumulated precipitation, on a 1km X 1km resolution map.

A mean bias correction scheme is applied and it is shown that the correction factor is very variable when it is computed using the rain gauge and radar pairs, collected for an hour of precipitation. The correction factor is more stable when the sample is increased by recording four days of hourly precipitation. The mean bias correction is so applied and verified versus an independent set of rain gauges. In many cases the statistical indices are improved. The algorithm removes precipitation bias for wide precipitating area and reduces a lot the heavy rain cores.

The non-uniform bias correction here presented draws on that of Koistinen and Puhakka (1981), but only the term based on gauge density is considered. The method follows intrinsic rain variability and better performs in most cases, especially in preserving the intensity of convective cells.

The two methods are implemented with different thresholds to select rainy pairs for merging radar and gauges. For the mean bias correction a threshold of 0.2 mm is chosen and no threshold on the number of available rainy points is imposed, on the other hand the non-uniform bias correction uses a threshold of 1 mm and a minimum number of points. This contributes to the stability of corrections, but also increases the time intermittency of corrected maps availability, since more often the non-uniform bias correction algorithm cannot be applied.

An issue for future work is to check the robustness of the methods, by calculating the verification indices with different subsets of rain gauges, firstly by reversing the two rain gauge datasets here used.

The two methods investigated in this work are aimed to meet different operational requirements. The mean bias correction is addressed mainly to correct quantitative precipitation radar estimates for longer time and spatial scales, for example for idrological or soil water balance models. The non-uniform bias correction has a fast response to precipitation field variability in time and it is more suitable for monitoring in real-time intense precipitation events. A key issue of merging gauges and radar techniques is the selection of the proper algorithm.

## Acknowledgment

This research was co-funded by the Italian National Civil Protection Department, under the contract “Modellistica meteorologica numerica finalizzata alla previsione meteorologica a brevissimo, breve e medio termine”, 2011-2013.

## References

Alberoni P. P., Anderson T., Mezzasalma P., Michelson D. B. and Nanni S., 2001: Use of the vertical reflectivity profile for identification of anomalous propagation. *Meteorological Applications*, **8**, 257-266

Barbosa S. 1994. Brief review of radar-raingauge adjustment techniques. *Almeida-Teixeira, M.E., Fantechi, R., Moore R. & Silva V.M. (eds.), Advances in radarhydrology, European Commission, EUR 14334 EN, Brussels*, 148–169

Bech, J., Codina, B., Lorente, J., Bebbington, D., 2003: The sensitivity of single polarization weather radar beam blockage correction to variability in the vertical refractivity gradient. *Journal of Atmospheric and Oceanic Technology*, **20**, 845-855

Brandes E.A., 1975: Optimizing rainfall estimates with the aid of radar. *J. Appl. Meteor.*, **14**,1339–1345

Chumchean S., Sharma A. And Seed A., 2006: An Integrated Approach to Error Correction for Real-Time Radar-Rainfall Estimation. *Journal of Atmospheric and Oceanic Technology*, **23**, 67-79

Goudenhoofdt E. and L. Delobbe, 2009: Evaluation of radar-gauge merging methods for quantitative precipitation estimates. *Hydrol. Earth Syst. Sci.*, **13**, 195–203

Fornasiero A., Bech J., and Alberoni P. P., 2006: Enhanced radar precipitation estimates using a combined clutter and beam blockage correction technique. *SRef-ID: 1684-9981/nhess/2006-6-697*, 697-710

Koistinen J. and Puhakka T., 1981: An improved spatial gauge-radar adjustment technique. *Proc. 20th Conf. On Radar Met. AMS*, 179–186